Carbohydrate Polymer Technologies and Applications 2 (2021) 100094

Contents lists available at ScienceDirect

Carbohydrate Polymer Technologies and Applications

journal homepage: www.elsevier.com/locate/carpta

A selective cellulose/hemicellulose green solvents extraction from buckwheat chaff

Daniela Caputo[a], Caterina Fusco[b], Angelo Nacci[a,b], Gerardo Palazzo[a,c], Sergio Murgia[c,d,e], Lucia D'Accolti[a,*], Luigi Gentile[a,c,**]

[a] Department of Chemistry, University of Bari "Aldo Moro", Via Orabona 4, Bari 70126, Italy
[b] ICCOM-CNR, Istituto di Chimica dei Composti Organometallici, Bari Section, Via Orabona 4, Bari 70125, Italy
[c] Center for Colloid and Surface Science (CSGI), Sesto Fiorentino, Italy
[d] Department of Chemical and Geological Sciences, University of Cagliari, Cagliari, Italy
[e] Department of Life and Environmental Sciences, University of Cagliari, Cagliari, Italy

ARTICLE INFO

Keywords:
Cellulose
Buckwheat chaff
Ionic liquids
Self-diffusion NMR
FTIR-ATR and TGA

ABSTRACT

A two-phase extraction process was adopted to obtain cellulose and hemicellulose from buckwheat chaff by using green solvents. We are proposing a combination of propylene carbonate (PC) and ionic liquids (ILs) in a 1:5 ratio. We compared the first-generation ILs 1-butyl-2,3-dimethylimidazolium chloride (BdmimCl), and 1-butyl-3-methyl imidazolium acetate (BmimAc) with respect to the tetrabutyl ammonium acetate (TBAAc). The cellulose and hemicellulose were, firstly, extracted into the PC/IL mixture and subsequently precipitated by water addition. All precipitate materials were analysed by FTIR-ATR and TGA, while the organic phase and the supernatant after water addition were analysed by using self-diffusion NMR. The PC green co-solvent was proven to be an exceptional candidate to replace dimethyl sulfoxide. The highest amount of precipitate material after water addition was obtained with PC-BmimAc, while PC-TBAAc was showing the highest cellulose/hemicellulose selectivity. Furthermore, a preferential interaction of the supernatant cellulose residue with PC or acetate was observed by self-diffusion NMR.

1. Introduction

Cellulose is the main substance that makes up the plant cell wall and contributes to the physical stability of the cells (Duchemin et al., 2012). Cellulose is traditionally employed as a raw material to produce paper, paperboard, fiberboard, and other similar products. Its peculiar chemical properties, including chirality, biodegradability, capacity for broad chemical modifications, and ability to form semi-crystalline fiber morphologies, have drawn considerably increasing interest and encouraged worldwide interdisciplinary research on this biopolymer and its derivatives over the past decades (Heinze & Liebert, 2012; Klemm, Heublein, Fink & Bohn, 2005; Moon, Martini, Nairn, Simonsen, & Youngblood, 2011; Siró & Plackett, 2010).

Traditionally, separation of cellulose from vegetable sources is conducted with procedures that employ toxic chemicals, such as the Kraft pulping process, which involves the separation of cellulose and hemicellulose from lignin using Na_2S and NaOH, or in presence of an acidic solution containing Na_2SO_3, sulphuric acid and cetrimonium bromide (CTAB) surfactant (Song, Ma & Xiang, 2019). Besides wood, cellulose can be extracted from many other natural sources, such as vegetable fibers including cotton, jute, flax, ramie, sisal, and hemp (Aranguren, Marcovich & Reboredo, 2016; Jahan, Saeed, He & Ni, 2011; Nazir, Wahjoedi, Yussof, & Abdullah, 2013). For instance, formic acid-based extraction process on jute fibers leads to cellulose, hemicellulose, and lignin yields of 59.8%, 76%, and 85.8%, respectively (Jahan et al., 2011). A cellulose yield of 60% was obtained from oil palm empty fruit bunches using a combination of formic acid (20%) and hydrogen peroxide (10%) (Nazir, Wahjoedi, Yussof, & Abdullah, 2013).

However, it is extremely difficult to dissolve cellulose in common organic solvents due to intermolecular hydrogen bonding between cellulose chains and to the hydrophobic properties (Medronho & Lindman, 2015). A limited number of solutes have been used for extracting cellulose in water, such as NaOH, tetrabutylammonium hydroxide, cuprammonium hydroxide, and cupriethylenediamine hydroxide (Budtova & Navard, 2016; Gentile & Olsson, 2016;

Abbreviations: FTIR-ATR, fourier transform infrared spectroscopy – attenuated total reflectance; NMR, nuclear magnetic resonance; TGA, thermal gravimetric analysis.

* Corresponding author.
** Corresponding author at: Department of Chemistry, University of Bari "Aldo Moro", Via Orabona 4, Bari 70126, Italy.
E-mail addresses: lucia.daccolti@uniba.it (L. D'Accolti), luigi.gentile@uniba.it (L. Gentile).

https://doi.org/10.1016/j.carpta.2021.100094
Received 29 April 2021; Received in revised form 21 May 2021; Accepted 24 May 2021
Available online 28 May 2021

Gubitosi, Duarte, Gentile, Olsson & Medronho, 2016; Hagman et al., 2017; Hoenich, Woffindin, Stamp, Roberts & Turnbull, 1997; Roy, Budtova & Navard, 2003).

Ionic liquids (ILs) are a class of solvents possessing many attractive properties, including good chemical and thermal stability, non-flammability, and immeasurable low vapor pressure. They have been considered as effective non-aqueous solvents capable of dissolving cellulose (Bhat, Khan, Usmani, Umapathi & Al-Kindy, 2019; Ciacco, Liebert, Frollini & Heinze, 2003; Idström et al., 2017; Kosan, Michels & Meister, 2008; Liu, Zhang, Sun, Bian & Hu, 2019; Swatloski, Spear, Holbrey & Rogers, 2002; Zavrel, Bross, Funke, Büchs & Spiess, 2009).

The dissolution mechanism of cellulose in ILs involves the oxygen and hydrogen atoms of cellulose-OH in the formation of electron donor-electron acceptor (EDA) complexes which interact with the ionic liquid (Myasoyedova, Zavyalov, Pokrovsky & Krestov, 1990). Currently, imidazolium salts are the best media in the dissolution of cellulose, probably because of the planar structure of the cation that stabilizes the polysaccharide polymer. However, especially if used as unique solvent, these ILs are difficult to handle because of their high viscosity, requiring high working temperature up to 130 °C for long times, i.e. from 40 to 240 min with final yields from 10% to 15% (Zhang, Wu, Zhang, & He, 2005; Zavrel et al., 2009; Xu, Wang, & Wang, 2010). Besides high viscosity, the low dissolution rate and the high costs are further drawbacks encountered when using ionic liquids. Finally, there are some indications of potentially hazardous properties of such salts (Swatloski, Holbrey & Rogers, 2003). These problems can be solved by adding aprotic polar co-solvents, which do not affect H-bonds in cellulose-IL interaction and decrease the solvent viscosity. To date, dimethyl sulfoxide (DMSO) (Ciacco et al., 2003; Idström et al., 2017; Wang, Li, Cao & Tang, 2011) and dimethylformamide (Dong, Takeshita, Miyafuji, Nokami & Itoh, 2018) have been used to this end, raising extraction yields of cellulose up to 18% respect to the pure ionic liquid. For instance, a cellulose yield of 62% was obtained from wood chip by using an extraction method based on 1-allyl-3-methylimidazolium chloride, and yield was further increased to 85% when dimethyl sulfoxide (DMSO) was employed as co-solvent (Wang et al., 2011). However, these strategies impose the drawback of using very toxic compounds that impedes industrial scale-up of method.

Here our working hypothesis is to exchange DMSO with another co-solvent with less impact on the environment, easy to handle, and with the ability to improve cellulose extraction. To our knowledge, there is only one attempt to use a combination of ionic liquids and propylene carbonate (PC) for cellulose dissolution, homogeneous processing, and derivatisation in which the extraction procedure was not investigated (Yuan et al., 2017). Here, for the first time, we are proposing a convenient and selective PC-ILs based extraction of cellulose/hemicellulose from buckwheat hulls an agro-food non-edible waste of vegetable origin. Lignin presence was below detectability in the cellulose/hemicellulose extracts. Moreover, we are presenting insight into the role of the PC in cellulose dissolution. The proposed extraction is a two-steps process that combines the advantages deriving from peculiar interactions exerted by ILs towards cellulose with the green solvent properties of propylene carbonate.

2. Materials and methods

2.1. Materials

Tetrabutylammonium acetate, 1-butyl-3-methylimidazolium acetate and propylene carbonate were purchased by Sigma-Aldrich, 1-butyl-2,3-dimethylimidazolium chloride was purchased by Fluka. All the reagents and solvents were used as received, without any further treatment. Lignin and cellulose microcrystalline powder were purchased by Sigma-Aldrich and used without further purification. Buckwheat chaff was kindly gifted of Puglia Industry.

2.2. Cellulose extraction procedure

The buckwheat chaff was crushed using an immersion blender; afterward the powder was dried at 60 °C in oven for 12 h. The extractive two-phase procedure was conducted according to a known procedure with some modification (Wang et al., 2011). In a round bottom flask, 500 mg of chaff were added into 9.5 g of a mixture of propylene carbonate/ionic liquid (1:5) and stirred for 10 min at 120 °C. Mixture was cooled at room temperature and centrifuged for 10 min at 4000 rpm (phase one). The supernatant organic phase was directly analysed by means of diffusion NMR to verify the presence of dissolved cellulose, while sediment was recovered, dried and weighted to calculate, by subtraction, the extracted amount of cellulose. Subsequently (phase two), water was added to the supernatant organic phase to precipitate cellulose that was separated and recovered by centrifugation. The aqueous phase was analysed by means of diffusion NMR to verify the presence of aggregates. The extracted cellulose was dried in oven at 50 °C and characterized by ATR-FTIR and thermogravimetric analysis (TGA) to investigate the composition and thermal stability of the extracted material.

2.3. Attenuated total reflectance-fourier transform infrared spectroscopy (ATR-FTIR)

The buckwheat chaff extracted materials were analysed by FTIR spectroscopy using a PerkinElmer Universal ATR (UATR) Two spectrophotometer equipped with a single reflection diamond ATR crystal (refractive index of 2.4). The spectra were recorded in the range between 400 and 4000 cm^{-1} with a resolution of 4 cm^{-1}. All the spectra were acquired in 32 scans applying the baseline correction and the ATR correction.

2.4. Thermogravimetric analysis (TGA)

The thermal stability of extracted cellulose was studied by a Perkin-Elmer Pyris 1 TGA (Thermogravimetric Analyzer) instrument. Both TGA and differential thermogravimetry (DTG) curves were measured. The samples were run at a heating rate of 10 °C/min in the range of 30–600 °C under continuous nitrogen flow. The thermogravimetric analysis allow to estimate the grade of purity of extracted cellulose and the residual lignin after the extraction.

2.5. ^1H and self-diffusion NMR

^1H and ^1H self-diffusion NMR measurements were performed on a 4.68 T Bruker 200 instrument equipped with a commercial diffusion probe (DIF-25 5 mm). All measurements were conducted at 25 ± 1°C and before each measurement the temperature was allowed to equilibrate for 5 min. ^1H NMR measurements were conducted using a 9.5 μs pulse and 32 scans. Self-diffusion measurements were conducted using a pulsed field gradient stimulated spin-echo (PGSTE) pulse sequence using a 9.5 μs ^1H pulse, 8 scans, and a 4.0 s relaxation delay. In the PGSTE sequence a pair of trapezoidal narrow magnetic field gradient pulses with amplitude g and duration δ encode for spin displacement over a controlled observation time Δ. By applying the pulsed magnetic field gradients along the z-direction the corresponding diffusion coefficient can be determined. The experimental conditions to measure H_2O self-diffusion coefficients were Δ = 140 ms, δ = 2 ms and g were varied from 6.2 to 25 G•cm^{-1} in 16 gradient steps for the aqueous phase, while and ionic liquids in the water phase Δ = 60 ms, δ = 2 ms and g were varied from 20 to 80 G•cm^{-1}. On the other hand in the organic phase ionic self-diffusion was measured with Δ = 60 ms, δ = 2 ms and g were varied from 175 to 700 G•cm^{-1}. The spin−echo decays were analysed according to Stejskal and Tanner (1965),

$$\ln\left(\frac{I}{I_0}\right) = -D\left[(\gamma\delta g)^2\left(\Delta - \frac{\delta}{3}\right)\right] = -Db \quad (1)$$

Table 1
Extracted material from buckwheat chaff using propylene carbonate (PC) and ionic liquids (ILs) mixture as green solvents.[a]

Ionic liquids	Labelling	Total yield of extracted materials (wt%)[b]	Yield of cellulose/hemicellulose (wt%)[c]
1-butyl-2,3-dimethylimidazolium chloride (1)	PC-BdmimCl	8	68
Tetrabutylammonium acetate (2)	PC-TBAAc	10	97
1-butyl-3-methyl imidazolium acetate (3)	PC-BmimAc	28	72

[a] Extracting procedure as reported in sect. 2.2.
[b] Determined gravimetrically and referred to initial weight of buckwheat chaff (sect. 2.3).
[c] Weight percentages of cellulose referred to regenerated materials evaluated by TGA analyses (Fig. 2).

Where I and I_0 represent the resonance peak intensity in the presence and absence of field gradients and γ is the proton gyro-magnetic ratio.

2.6. Gravimetric determination of total amount of the extracted materials

The procedure is based on the variation of the weight of the buckwheat chaff after the extraction process. Exactly 10 g of buckwheat husk powder are weighed after drying in a stove inside an aluminium weighing boats, previously brought to constant weight. After the extraction procedure, the residual chaff is dried again with same procedure. The overall yield of extracted material is calculated according to the following formula: Yield (%) = $[(A\text{-}B)/A] \times 100$, where A is the weight of the sample in the aluminium weighing boats before extraction. B is the weight of the sample in the aluminium weighing boats after extraction. Three replicates are made for each sample.

3. Results and discussion

Investigations started with evaluation of the extraction capacity of mixtures composed by propylene carbonate and three selected ionic liquids: 1-butyl-2,3-dimethylimidazolium chloride, tetrabutylammonium acetate and 1-butyl-3-methyl imidazolium acetate. Each PC/IL extracting mixture was analysed by ^{1}H self-diffusion NMR measurements to estimate and characterize extracted materials, then subjected to water addition to regenerate cellulose/hemicellulose by precipitation. After centrifugation, the recovered materials were dried at 60 °C and analysed by attenuated total reflectance-Fourier transform infrared spectroscopy (ATR-FTIR) (see sect. 2.3), and TGA analysis (see sect. 2.4) to prove cellulose/hemicellulose extraction.

Yields of materials are reported in Table 1 for three PC/ILs mixtures. From results emerged that PC-BmimAc is the most powerful extracting solvent, furnishing the highest yield (28%), while PC-TBAAc showed a lower extracting capacity but a very high selectivity towards cellulose.

FTIR-ATR and thermogravimetric analyses were performed to identify the main chemical components of the extracted materials. Fig. 1 reports the FTIR spectra of the raw buckwheat chaff along with those of extracted substances obtained from the three PC/ILs solvent mixtures after regeneration from water. The absorption peaks observed in the region of 3600–3000 cm^{-1} correspond to the stretching vibrations of hydroxyl groups (-OH) (Manimaran, Senthamaraikannan, Sanjay, Marichelvam & Jawaid, 2018; Zhuang, Li, Pu, Ragauskas & Yoo, 2020; Zugenmaier, 2008), in the case of buckwheat chaff are mainly cellulose, hemicellulose and lignin. However, the peak at 3175 cm^{-1} is a strong indication of cellulose II presence (Yang, Zhang, Lang & Yu, 2017). Cellulose II has an antiparallel orientation between the chains instead of the parallel one of cellulose I. Precipitation of cellulose II has been recently suggested to occur in strong alkaline system (Gubitosi et al., 2016; Pereira et al., 2018). The peaks observed at 2919 cm^{-1} and 2850 cm^{-1} in the spectra are assigned to the CH_2 asymmetric and symmetric stretching, respectively, as a consequence can be attributed either to cellulose, hemicellulose or lignin.

The peak at 1727 cm^{-1} could be attributed to the waxy C=O acetyl group of hemicellulose ester or carbonyl ester of the lignin unit (Sisak, Daik & Ramli, 2015). Li, Li and Zhang (2002) reported an increase in the peak at 1720 cm^{-1} (attributed to C=O bonds in lignin) as a consequence of heat degradation of lignin in hardwood and softwood and obtained. The peak at 1640 cm^{-1} corresponding to the stretching and bending modes of the surface hydroxyls of cellulose (Jia, Li, Ma, Zhu & Sun, 2011), while the peak at 1598 cm^{-1} could be attributed to C=O stretching vibration in conjugated carbonyl of lignin (Kubovský, Kačíková & Kačík, 2020). The assignment of the peaks at 1640 cm^{-1} and at 1598 cm^{-1} to cellulose and lignin, respectively can be appreciated in Fig. S1 where microcrystalline cellulose and commercial lignin spectra are reported for comparison. The peak at 1512 cm^{-1} is usually associated with guaiacyl and syringyl units in wood lignin (Kubovský et al., 2020). The peak at 1371 cm^{-1} is due to C-H bending, C-H stretching in CH_3 as a consequence can arise from cellulose, hemicellulose or lignin (Zhuang et al., 2020). On the other hand, the peaks at 1275 cm^{-1} and 1261 cm^{-1} corresponds to bending vibration of C-O and C-H bending vibration in cellulose II, respectively (Ranganagowda, Kamath & Bennehalli, 2019).

The peak at 1161 cm^{-1} is usually attributes to C–O–C vibrations in cellulose and hemicelluloses. C–O stretching and C–O–C glycosidic bond stretching are attested by strong band at 1023 cm^{-1}, that along with the C-O-C anti symmetric stretching vibrations of ester group at 1240 cm^{-1} are typically attributed to cellulose (Peng, Wang, Ohkoshi & Zhang, 2015). Finally, the 893 cm^{-1} is assigned to group C1 frequency in cellulose II (Kumar, Singh Negi, Choudhary & Kant Bhardwaj, 2020). The FTIR-ATR spectra indicate the presence of cellulose, hemicellulose

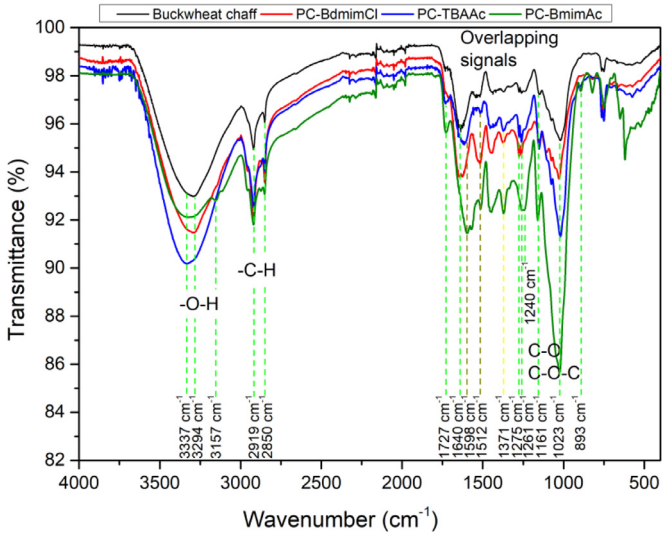

Fig. 1. FTIR-ATR spectra of the raw buckwheat chaff and the extracted materials obtained with propylene carbonate/1-butyl-2,3-dimethylimidazolium chloride (PC-BdmimCl), propylene carbonate/tetrabutylammonium acetate (PC-TBAAc), and propylene carbonate/1-butyl-3-methyl imidazolium acetate (PC-BmimAc) extraction media. The dotted green lines are indicating peaks coming mainly from cellulose or hemicellulose, while the brown dotted lines are indicating peaks due to lignin, finally, the yellow dotted line is indicating a peak that could be due to cellulose, hemicellulose, or lignin (For interpretation of the references to color in this figure legend, the reader is referred to the web version of this article.).

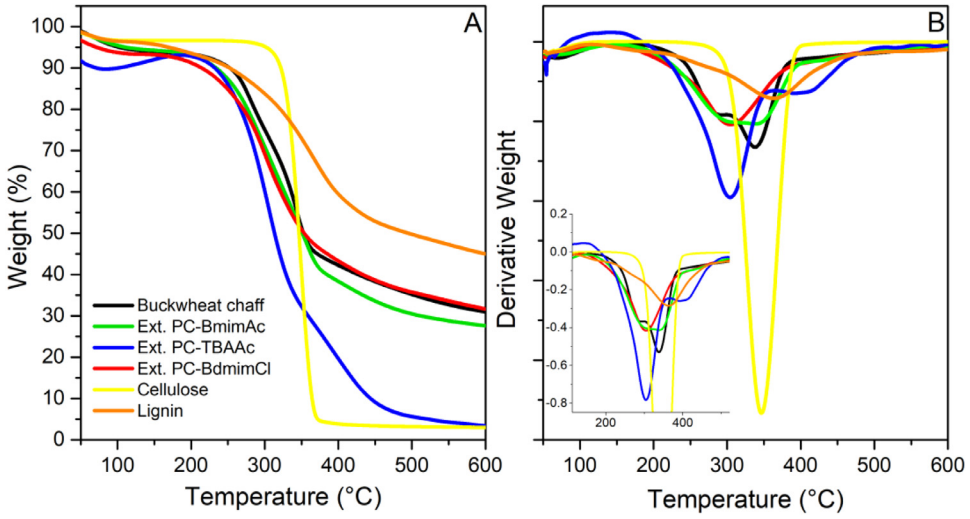

Fig. 2. Thermogravimetric analysis, TGA, curves (A) and derivative thermogravimetric, DTG, profiles (B) of the extracted materials obtained with propylene carbonate and 1-butyl-2,3-dimethylimidazolium chloride (PC-BdmimCl), propylene carbonate and tetrabutylammonium acetate (PC-TBAAc), propylene carbonate and 1-butyl-3-methyl imidazolium acetate (PC-BmimAc) extraction media as well as microcrystalline cellulose and lignin.

and lignin as expected. The higher intensity of the cellulose peak at 1023 cm^{-1} for the material extracted with PC-BmimAc respect to the other extractions indicate a higher content of cellulose. Furthermore, the presence of cellulose II was detected in all extracted materials, even though the peak at 3157 cm^{-1} was evident only for the PC-BmimAc extraction.

Thermogravimetric analysis was conducted to investigate the composition of regenerated material and calculate the amount of cellulose/hemicellulose obtained after the extraction. All the thermal degradation curves (Fig. 2A) show an initial weight loss in the range of 60–100 °C due to the release of moisture. A greater loss of water was observed for the extraction with PC-TBAAc because of its increased hygroscopic properties. All the samples show an initial onset temperature at 200 °C, while the DTG decomposition curves show peaks at 305 °C for PC-TBAAc, at 301 °C for PC-BdmimCl and at 336 °C for PC-BmimAc suggesting the presence of crystalline cellulose (Fig. 2B). Fig. 2 reports microcrystalline cellulose and commercial lignin as references. All the samples present the offset temperature (T_{offset}) at about 500 °C due to the degradation of high molecular weight lignin. However, at this temperature, it is possible to observe, a weight losses of 70 %, 95% and 64% for the extraction with PC-BmimAc, PC-TBAAc and PC-BdmimCl, respectively.

^{1}H NMR spectra and ^{1}H self-diffusion NMR were adopted to understand the dissolution process of cellulose in ionic liquids and other solvents such as tetrabutylammonium hydroxide and NaOH in water (Gentile & Olsson, 2016; Hagman et al., 2017; Idström et al., 2017). ^{1}H NMR resonances of cellulose in ionic liquids are reported in the 2–4 ppm region (Kuroda, Kunimura, Fukaya & Ohno, 2014), while ^{1}H self-diffusion NMR of the ionic liquids were used to highlight the interactions with the cellulose (Idström et al., 2017). Here, ^{1}H NMR spectroscopy was used for evaluating the efficiency of regeneration by analysing extracting solvent before and after water addition, i.e. ^{1}H NMR spectra were collected for the organic phase (step one) and the water phase (step two). All proton NMR spectra of PC/ILs mixtures after regeneration (step two) is dominated by the water peak, which overcomes any cellulose/hemicellulose resonance (see supplementary data) even though molecularly dissolved cellulose is not expected due the precipitation in water presence. Fig. 3 reports the ^{1}H NMR spectra and ^{1}H self-diffusion NMR experiments (echo decays) on the PC-BdmimCl and PC-TBAAc organic phases, while Fig. 4 reports the corresponding data relative to the PC-BmimAc organic phase (step one). The ^{1}H NMR spectrum of the PC-BdmimCl organic phase (Fig. 3A) reveals the presence of propylene carbonate (PC) peaks that overlaps with cellulose signals. The echo-decays on three chemical shift regions were monitored to detect cellulose/hemicellulose presence (Fig. 3B). Table 2 reports all the

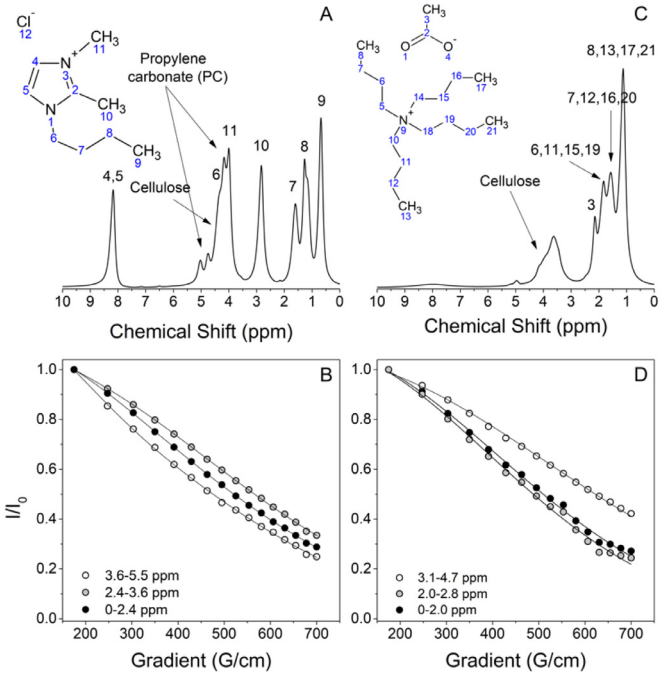

Fig. 3. ^{1}H NMR spectra (A, C) and ^{1}H self-diffusion NMR echo-decays (B, D) of the organic PC-BdmimCl (A,B) and PC-TBAAc (C, D) phase supernatant. The echo-decays are related to 3 chemical shift regions listed in Table 2 for PC-BdmimCl and PC-TBAAc. The black lines on the echo-decays are mono-exponential fitting (Eq. (1)) except for the 3.6–5.5 ppm region of PC-BdmimCl for which a bi-exponential fitting was adopted.

self-diffusion values obtained for the investigated systems and for the pure PC-ILs extraction solvents. All diffusion coefficients are slower than the pure solvent for the PC-BdmimCl organic phase. The only exception is an IL impurity (resonance in the 3.6–5.5 ppm region) that accounts for a fast-phase in the echo decay; however, this is a minor contribution of the decay (~8%) and should not be considered. Interestingly, the PC diffusion coefficient is the most affected in the PC-BdmimCl and partially in the PC-BmimAc indicating cellulose/hemicellulose-PC interactions, while ILs act as a solvent matrix. Notably, the PC signal is not detectable in the PC-TBAAc organic phase and in the pure PC-TBAAc solvent, probably due to extremely short relaxation time due to interactions with the IL. The diffusion coefficient of TBA^+ in the PC-TBAAc increases

Table 2
^{1}H NMR self-diffusion coefficients of the PC-ILs organic phase (first extraction step), pure ILs solvents, and the water phase (second extraction step).

(PC-IL) extraction phase	Chemical Shift region (ppm) *1st step*	Assignment	Self-Diffusion (m^2/s)	Self-Diffusion of the pure PC-ILs mixtures (m^2/s)	Chemical Shift region (ppm) *2nd step*	Assignment	Self-Diffusion (m^2/s)
PC-BdmimCl	0-2.4	Ionic liquid	$(1.6 \pm 0.1)10^{-12}$	$(1.9 \pm 0.1)10^{-12}$	0–3	Ionic liquid	$(9.2 \pm 0.2)10^{-10}$
	2.4-3.6	Ionic liquid	$(1.4 \pm 0.2)10^{-12}$	$(1.9 \pm 0.1)10^{-12}$	4.8	Water	$(2.5 \pm 0.1)10^{-9}$
	3.6-5.5	PC and/or Cellulose	$(1.6 \pm 0.2)10^{-12}$	$(5.2 \pm 0.2)10^{-12}$			
			$(1.1 \pm 0.1)10^{-11}$*	$(1.9 \pm 0.1)10^{-11}$*			
PC-TBAAc	0-2.0	Ionic liquid	$(1.7 \pm 0.1)10^{-12}$	$(3.1 \pm 0.1)10^{-13}$	0–3	Ionic liquid	$(5.6 \pm 0.2)10^{-10}$
	2.0-2.8	IL acetate anion	$(1.9 \pm 0.1)10^{-12}$	$(1.6 \pm 0.1)10^{-12}$	4.8	Water	$(2.3 \pm 0.1)10^{-9}$
				$(3.1 \pm 0.1)10^{-13}$			
	3.1-4.7	PC and/or Cellulose	$(9.9 \pm 0.2)10^{-13}$	X			
PC-BmimAc	0.2-1.6	Ionic liquid	$(4.9 \pm 0.2)10^{-12}$	$(4.3 \pm 0.1)10^{-12}$	0–3	Ionic liquid	$(9.4 \pm 0.2)10^{-10}$
	1.6-2.0	IL acetate anion	$(5.0 \pm 0.2)10^{-12}$	$(5.3 \pm 0.1)10^{-12}$	4.8	Water	$(2.5 \pm 0.1)10^{-9}$
	3.2-5.4	PC and/or Cellulose	$(4.8 \pm 0.2)10^{-12}$	$(5.5 \pm 0.1)10^{-12}$			

* Diffusion coefficients attributed to impurities.

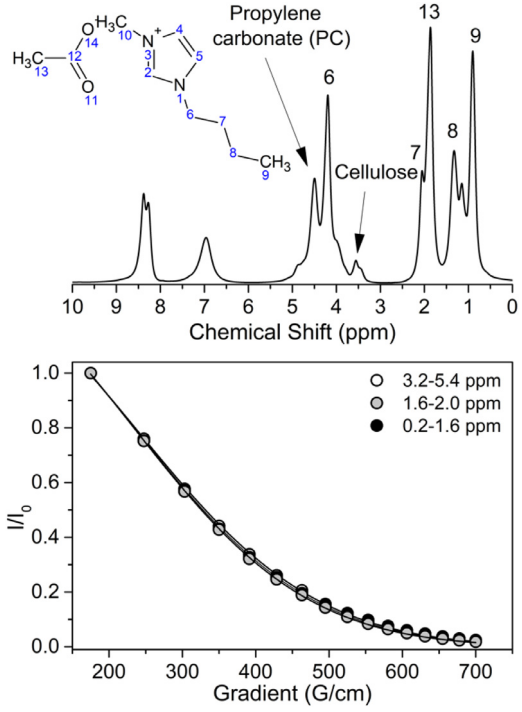

Fig. 4. ^{1}H NMR spectra (A) and ^{1}H self-diffusion NMR echo-decays (B) of the organic PC-BmimAc phase supernatant. The echo-decays are related to 3 chemical shift regions listed in Table 2. The black lines on the echo-decays are mono-exponential fitting (Eq. (1)).

by almost an order of magnitude in presence of cellulose/hemicellulose with respect to the pure solvent. Usually, the solvent self-diffusion coefficients decrease with increasing obstruction, i.e., increasing solute content or size (Murgia, Palazzo, Mamusa, Lampis & Monduzzi, 2009). However, the obstruction effect has been demonstrated to be inadequate to explain the strong decrease of the solvent diffusion with cellulose amount (Gentile & Olsson, 2016) indicating an interaction between solvent and cellulose. The faster diffusion coefficient of TBA^+ can be interpreted as cellulose/hemicellulose interaction with the acetate group, as observed by Idström et al. for cellulose in the TBAAc/DMSO system (Idström et al., 2017).

The lignin was not detected in the ^{1}H NMR; as a consequence, its impact on the diffusion of the solvent (if any) cannot be quantified and in the following we will ascribe the slowing down in the solvent components only to the presence of cellulose and hemicellulose.

Based on results in Table 1 and considering and ^{1}H self-diffusion NMR echo-decays experiments, it can be argued that structure of both ions of ILs play an important role in the extraction process. In particular, imidazolium cations of BdmimCl and BmimAc seem to be responsible mainly of extraction of lignin fraction, by virtue of their aromatic nature that can form π-interactions with that polyphenol polymer. In contrast, in the case of tetrabutylammonium cations the bulky aliphatic chains shield positive charge on nitrogen impeding any interactions with solutes, as highlighted by self-diffusion coefficients of TBA^+. Therefore, in this case, extraction capacity should be due exclusively to acetate anions, and particularly to their H-bond accepting ability (Dong, Zhang & Wang, 2016). This could explain the high selectivity exhibited by TBAAc towards polysaccharide cellulose.

4. Conclusions

Here we demonstrated the efficiency of a cellulose two-phase extraction process from buckwheat chaff by using propylene carbonate (PC) and ionic liquids (ILs) as green solvents in the 1:5 ratio. Three different ILs were adopted to compare extraction performance: 1-butyl-2,3-dimethylimidazolium chloride (BdmimCl), 1-butyl-3-methyl imidazolium acetate (BmimAc), and tetrabutylammonium acetate (TBAAc). Water was added to the extracting organic phases to precipitate cellulose and hemicellulose and the resulting materials were analysed by FTIR-ATR and TGA, compared with the original source, showing the presence of both cellulose and lignin. The highest amount 28% of extracted material was obtained with PC-BmimAc. However, the more efficient extraction in terms of selectivity was obtained with the mixture PC-TBAAc, where the amount of extracted material was only 10 wt%, but entirely composed of cellulose with a high degree of purity, as demonstrated by the thermogravimetric analysis. Furthermore, the presence of cellulose II in the precipitated material was detected. Finally, the supernatants obtained after the extraction process were analysed by using self-diffusion NMR. We noticed that cellulose/hemicellulose interacts preferentially with PC in the case of PC-BdmimCl and PC-BmimAc, while interacting preferentially with the acetate group in the case of PC-TBAAc. DMSO substitution with PC was a successful working hypothesis even though PC does not mediate the dissolution, on the contrary, was promoting acetate interaction in the PC-TBAAc system. The PC-TBAAc system can be considered a selective eco-friendly extraction media.

Declaration of Competing Interest

We have no conflict of interests.

Acknowledgment

This work is partially supported by funds from European Union-19 FESR "PON Ricerca e Innovazione 2014–2020. Progetto: 20 Energie per l'Ambiente TARANTO-Cod. ARS01_00637" and POR Puglia FESR 2014-2020—Azione 1.6 Bando "INNONETWORK 2017" Progetto HOQ3PM3 "MOSAICOS-MOSAici Interattivi eCO-Sostenibili". Thanks to CNR-ICCOM for the Fund PIANI di SVILUPPO INDUSTRIALI attraverso PACCHETTI INTEGRATI di AGEVOLAZIONE (PIA) Regione Basilicata codice progetto 227179".

Declarations

Funding: This work is partially supported by funds from European Union-19 FESR "PON Ricerca e Innovazione 2014–2020. Progetto: 20 Energie per l'Ambiente TARANTO-Cod. ARS01_00637" and POR Puglia FESR 2014-2020—Azione 1.6 Bando "INNONETWORK 2017" Progetto HOQ3PM3 "MOSAICOS-MOSAici Interattivi eCO-Sostenibili". Thanks to CNR-ICCOM for the Fund PIANI di SVILUPPO INDUSTRIALI attraverso PACCHETTI INTEGRATI di AGEVOLAZIONE (PIA) Regione Basilicata codice progetto 227179".

Availability of data and material

Data are included in the manuscript and supplementary data.

Code availability

'Not applicable'.

Ethics approval

'Not applicable'.

Supplementary materials

Supplementary material associated with this article can be found, in the online version, at doi:10.1016/j.carpta.2021.100094.

References

Aranguren, M. I., Marcovich, N. E., & Reboredo, M. M. (2016). Vegetable fibers. In *Encyclopedia of Polymer Science and Technology* (pp. 1–26). Hoboken, NJ, USA: John Wiley & Sons, Inc. https://doi.org/10.1002/0471440264.pst380.pub2.

Bhat, A. H., Khan, I., Usmani, M. A., Umapathi, R., & Al-Kindy, S. M. Z (2019). Cellulose an ageless renewable green nanomaterial for medical applications: An overview of ionic liquids in extraction, separation and dissolution of cellulose. *International Journal of Biological Macromolecules* Elsevier B.V.. https://doi.org/10.1016/j.ijbiomac.2018.12.190.

Budtova, T., & Navard, P. (2016). Cellulose in NaOH–water based solvents: A review. *Cellulose, 23*(1), 5–55. https://doi.org/10.1007/s10570-015-0779-8.

Ciacco, G. T., Liebert, T. F., Frollini, E., & Heinze, T. J. (2003). Application of the solvent dimethyl sulfoxide/tetrabutyl-ammonium fluoride trihydrate as reaction medium for the homogeneous acylation of Sisal cellulose. *Cellulose, 10*(2), 125–132. https://doi.org/10.1023/A:1024064018664.

Dong, K., Zhang, S., & Wang, J. (2016). Understanding the hydrogen bonds in ionic liquids and their roles in properties and reactions. *Chemical Communications, 52*(41), 6744–6764. https://doi.org/10.1039/c5cc10120d.

Dong, Y., Takeshita, T., Miyafuji, H., Nokami, T., & Itoh, T. (2018). Direct extraction of polysaccharides from moso bamboo (Phylostachys heterocycla) chips using a mixed solvent system of an amino acid ionic liquid with polar aprotic solvent. *Bulletin of the Chemical Society of Japan, 91*(3), 398–404. https://doi.org/10.1246/bcsj.20170383.

Duchemin, B., Thuault, A., Vicente, A., Rigaud, B., Fernandez, C., & Eve, S. (2012). Ultrastructure of cellulose crystallites in flax textile fibres. *Cellulose, 19*(6), 1837–1854. https://doi.org/10.1007/s10570-012-9786-1.

Gentile, L., & Olsson, U. (2016). Cellulose–solvent interactions from self-diffusion NMR. *Cellulose, 23*(4). https://doi.org/10.1007/s10570-016-0984-0.

Gubitosi, M., Duarte, H., Gentile, L., Olsson, U., & Medronho, B. (2016). On cellulose dissolution and aggregation in aqueous tetrabutylammonium hydroxide. *Biomacromolecules*, (9), 17. https://doi.org/10.1021/acs.biomac.6b00696.

Hagman, J., Gentile, L., Jessen, C. M., Behrens, M., Bergqvist, K. E., & Olsson, U. (2017). On the dissolution state of cellulose in cold alkali solutions. *Cellulose, 24*(5), 2003–2015. https://doi.org/10.1007/s10570-017-1272-3.

Heinze, T., & Liebert, T. (2012). Celluloses and polyoses/hemicelluloses. In *Polymer Science: A Comprehensive Reference, 10 Volume Set: 10* (pp. 83–152). Elsevier. https://doi.org/10.1016/B978-0-444-53349-4.00255-7.

Hoenich, N. A., Woffindin, C., Stamp, S., Roberts, S. J., & Turnbull, J. (1997). Synthetically modified cellulose: An alternative to synthetic membranes for use in haemodialysis? *Biomaterials, 18*(19), 1299–1303. https://doi.org/10.1016/S0142-9612(97)00062-8.

Idström, A., Gentile, L., Gubitosi, M., Olsson, C., Stenqvist, B., Lund, M., & Bialik, E. (2017). On the dissolution of cellulose in tetrabutylammonium acetate/dimethyl sulfoxide: a frustrated solvent. *Cellulose*. https://doi.org/10.1007/s10570-017-1370-2.

Jahan, M. S., Saeed, A., He, Z., & Ni, Y. (2011). Jute as raw material for the preparation of microcrystalline cellulose. *Cellulose, 18*(2), 451–459. https://doi.org/10.1007/s10570-010-9481-z.

Jia, N., Li, S. M., Ma, M. G., Zhu, J. F., & Sun, R. C. (2011). Synthesis and characterization of cellulose-silica composite fiber in ethanol/water mixed solvents. *BioResources, 6*(2), 1186–1195. https://doi.org/10.15376/biores.6.2.1186-1195.

Klemm, D., Heublein, B., Fink, H. P., & Bohn, A. (2005). Cellulose: Fascinating biopolymer and sustainable raw material. *Angewandte Chemie - International Edition* John Wiley & Sons, Ltd. https://doi.org/10.1002/anie.200460587.

Kosan, B., Michels, C., & Meister, F. (2008). Dissolution and forming of cellulose with ionic liquids. *Cellulose, 15*(1), 59–66. https://doi.org/10.1007/s10570-007-9160-x.

Kubovský, I., Kačíková, D., & Kačík, F. (2020). Structural changes of oak wood main components caused by thermal modification. *Polymers, 12*(2). https://doi.org/10.3390/polym12020485.

Kumar, A., Singh Negi, Y., Choudhary, V., & Kant Bhardwaj, N. (2020). Characterization of cellulose nanocrystals produced by acid-hydrolysis from sugarcane bagasse as agro-waste. *Journal of Materials Physics and Chemistry, 2*(1), 1–8. https://doi.org/10.12691/jmpc-2-1-1.

Kuroda, K., Kunimura, H., Fukaya, Y., & Ohno, H. (2014). 1H NMR analysis of cellulose dissolved in non-deuterated ionic liquids. *Cellulose, 21*(4), 2199–2206. https://doi.org/10.1007/s10570-014-0271-x.

Li, J., Li, B., & Zhang, X. (2002). Comparative studies of thermal degradation between larch lignin and manchurian ash lignin. *Polymer Degradation and Stability, 78*(2), 279–285. https://doi.org/10.1016/S0141-3910(02)00172-6.

Liu, R., Zhang, J., Sun, S., Bian, Y., & Hu, Y. (2019). Dissolution and recovery of cellulose from pine wood bits in ionic liquids and a co-solvent component mixed system. *Journal of Engineered Fibers and Fabrics, 14*, Article 155892501983844. https://doi.org/10.1177/1558925019838440.

Manimaran, P., Senthamaraikannan, P., Sanjay, M. R., Marichelvam, M. K., & Jawaid, M. (2018). Study on characterization of Furcraea foetida new natural fiber as composite reinforcement for lightweight applications. *Carbohydrate Polymers, 181*, 650–658. https://doi.org/10.1016/j.carbpol.2017.11.099.

Medronho, B., & Lindman, B. (2015). Brief overview on cellulose dissolution/regeneration interactions and mechanisms. *Advances in Colloid and Interface Science, 222*, 502–508. https://doi.org/10.1016/j.cis.2014.05.004.

Moon, R. J., Martini, A., Nairn, J., Simonsen, J., & Youngblood, J. (2011). Cellulose nanomaterials review: Structure, properties and nanocomposites. *Chemical Society Reviews, 40*(7), 3941–3994. https://doi.org/10.1039/c0cs00108b.

Murgia, S., Palazzo, G., Mamusa, M., Lampis, S., & Monduzzi, M. (2009). Aerosol-OT forms oil-in-water spherical micelles in the presence of the ionic liquid bmimBF4. *Journal of Physical Chemistry B, 113*(27), 9216–9225. https://doi.org/10.1021/jp902970n.

Myasoyedova, V. V., Zavyalov, N. A., Pokrovsky, S. A., & Krestov, G. A. (1990). Thermochemical characteristics of solutions of cellulose and its ethers and esters. *Thermochimica Acta, 169*(C), 111–119. https://doi.org/10.1016/0040-6031(90)80138-O.

Nazir, M. S., Wahjoedi, B. A., Yussof, A. W., & Abdullah, M. A. (2013). Eco-friendly extraction and characterization of cellulose from oil palm empty fruit bunches.. *BioResources, 8*(2), 2161–2172. https://doi.org/10.15376/biores.8.2.2161-2172.

Peng, W., Wang, L., Ohkoshi, M., & Zhang, M. (2015). Separation of hemicelluloses from eucalyptus species: Investigating the residue after alkaline treatment. cellulose chemistry and technology. *Cellulose Chemistry and Technology, 49*.

Pereira, A., Duarte, H., Nosrati, P., Gubitosi, M., Gentile, L., Romano, A., & Olsson, U. (2018). Cellulose gelation in NaOH solutions is due to cellulose crystallization. *Cellulose*. https://doi.org/10.1007/s10570-018-1794-3.

Ranganagowda, R. P. G., Kamath, S. S., & Bennehalli, B. (2019). Extraction and characterization of cellulose from natural areca fiber. *Material Science Research India, 16*(1), 86–93. https://doi.org/10.13005/msri/160112.

Roy, C., Budtova, T., & Navard, P. (2003). Rheological properties and gelation of aqueous cellulose–NaOH solutions. *Biomacromolecules, 4*(2), 259–264. https://doi.org/10.1021/bm020100s.

Siró, I., & Plackett, D. (2010). Microfibrillated cellulose and new nanocomposite materials: A review. *Cellulose* Springer. https://doi.org/10.1007/s10570-010-9405-y.

Sisak, M. A. A., Daik, R., & Ramli, S. (2015). Characterization of cellulose extracted from oil palm empty fruit bunch. *AIP Conference Proceedings, 1678* Vol.American Institute of Physics Inc. https://doi.org/10.1063/1.4931295.

Song, C., Ma, C., & Xiang, D. (2019). Variations in accumulation of lignin and cellulose and metabolic changes in seed hull provide insight into dehulling characteristic of tartary buckwheat seeds. *International Journal of Molecular Sciences, 20*(3), 524. https://doi.org/10.3390/ijms20030524.

Stejskal, E. O., & Tanner, J. E. (1965). Spin diffusion measurements: Spin echoes in the presence of a time dependent field gradient. *The Journal of Chemical Physics, 42*, 288. https://doi.org/10.1063/1.1695690.

Swatloski, R. P., Holbrey, J. D., & Rogers, R. D. (2003). Ionic liquids are not always green: Hydrolysis of 1-butyl-3- methylimidazolium hexafluorophosphate. *Green Chemistry, 5*(4), 361–363. https://doi.org/10.1039/b304400a.

Swatloski, R. P., Spear, S. K., Holbrey, J. D., & Rogers, R. D. (2002). Dissolution of cellose with ionic liquids. *Journal of the American Chemical Society, 124*(18), 4974–4975. https://doi.org/10.1021/ja025790m.

Wang, X., Li, H., Cao, Y., & Tang, Q. (2011). Cellulose extraction from wood chip in an ionic liquid 1-allyl-3-methylimidazolium chloride (AmimCl). *Bioresource Technology, 102*(17), 7959–7965. https://doi.org/10.1016/j.biortech.2011.05.064.

Xu, A., Wang, J., & Wang, H. (2010). Effects of anionic structure and lithium salts addition on the dissolution of cellulose in 1-butyl-3-methylimidazolium-based ionic liquid solvent systems.. *Green Chemistry, 12*(2), 268–275. https://doi.org/10.1039/b916882f.

Yang, Y. P., Zhang, Y., Lang, Y. X., & Yu, M. H. (2017). Structural ATR-IR analysis of cellulose fibers prepared from a NaOH complex aqueous solution. *IOP Conference Series: Materials Science and Engineering, 213*, Article 012039 Institute of Physics Publishing. https://doi.org/10.1088/1757-899X/213/1/012039.

Yuan, X., Yuan, C., Shi, W., Chen, P., Chen, H., Xie, H., & Zheng, Q. (2017). Propylene carbonate based-organic electrolytes for cellulose dissolution processing and derivatization. *ChemistrySelect, 2*(13), 3783–3787. https://doi.org/10.1002/slct.201700535.

Zavrel, M., Bross, D., Funke, M., Büchs, J., & Spiess, A. C. (2009). High-throughput screening for ionic liquids dissolving (ligno-)cellulose. *Bioresource Technology, 100*(9), 2580–2587. https://doi.org/10.1016/j.biortech.2008.11.052.

Zhang, H., Wu, J., Zhang, J., & He, J. (2005). 1-allyl-3-methylimidazolium chloride room temperature ionic liquid: A new and powerful nonderivatizing solvent for cellulose.. *Macromolecules, 38*(20), 8272–8277. https://doi.org/10.1021/ma0505676.

Zhuang, J., Li, M., Pu, Y., Ragauskas, A. J., & Yoo, C. G. (2020). Observation of potential contaminants in processed biomass using fourier transform infrared spectroscopy. *Applied Sciences, 10*(12) (Switzerland). https://doi.org/10.3390/app10124345.

Zugenmaier, P. (2008). *Crystalline Cellulose and Derivatives*. Berlin, Heidelberg: Springer Berlin Heidelberg. https://doi.org/10.1007/978-3-540-73934-0.